BASIC SCIENCE

Nanomedicine: Nanotechnology, Biology, and Medicine
13 (2017) 2633–2642

nanomedicine
Nanotechnology, Biology, and Medicine

Original Article

nanomedjournal.com

Biocompatibility assessment of silk nanoparticles: hemocompatibility and internalization by human blood cells

Manfred F. Maitz, MD[a], Claudia Sperling, PhD[a], Thidarat Wongpinyochit, MRes[b], Manuela Herklotz, PhD[a], Carsten Werner, PhD[a,*], F. Philipp Seib, PhD[a,b,**]

[a]*Leibniz Institute of Polymer Research Dresden, Max Bergmann Center of Biomaterials Dresden, Dresden, Germany*
[b]*Strathclyde Institute of Pharmacy and Biomedical Sciences, University of Strathclyde, Glasgow, UK*

Received 28 May 2017; accepted 17 July 2017

Abstract

Many nanoparticles are designed for use as potential nanomedicines for parenteral administration. However, emerging evidence suggests that hemocompatibility is important, but is highly particle- and test-bed dependent. Thus, knowledge of bulk material properties does not predict the hemocompatibility of uncharacterized nanoparticles, including silk nanoparticles. This study compares the hemocompatibility of silk versus silica nanoparticles, using whole human blood under quasi-static and flow conditions. Substantial hemocompatibility differences are noted for some nanoparticles in quasi-static versus dynamic studies; i.e., the inflammatory response to silk nanoparticles is significantly lower under flow versus quasi-static conditions. Silk nanoparticles also have very low coagulant properties - an observation that scales from the macro- to the nano-level. These nanoparticle hemocompatibility studies are complemented by preliminary live cell measurements to evaluate the endocytosis and trafficking of nanoparticles in human blood cells. Overall, this study demonstrates that nanoparticle hemocompatibility is affected by several factors, including the test bed design.

Key words: Silk; Fibroin; Silica; Blood compatibility

Nanoparticles for drug delivery were introduced in the 1970s; Abraxane® (albumin-paclitaxel nanoparticle) was the first-in-class drug delivery nanoparticle to entered routine clinical use in 2005.[1] This success has renewed interest in (protein) nanoparticles as drug delivery agents, and numerous nanoparticles are currently in clinical trials for a broad range of indications, including cancer.[2] Nanoparticles are attractive for anticancer drug delivery because the endothelium within a solid tumor is disorganized and leaky, while the tumor itself typically has poor lymphatic drainage. These factors result in an enhanced permeability and retention (EPR) of parenterally administered nanomedicine within solid tumors.[3,4]

However, the ability of a nanomedicine to exploit the EPR effect for tumor targeting depends on nanoparticle persistence in the blood circulation, minimal blood activation (i.e. coagulation and inflammation), absence of hemolysis and avoidance of clearance by circulating monocytes and granulocytes or the reticuloendothelial system of liver, spleen, and bone marrow.[5,6] One common approach for exploiting the EPR effect and minimizing clearance by immune cells is to surface decorate

Abbreviations: EPR, enhanced permeability and retention; PEG, poly(ethylene glycol); LPS, lipopolysaccharides; PF4, platelet factor 4.

Funders: This research was supported in part by a TENOVUS Scotland Grant S13/8 and Marie Curie FP7 Career Integration Grant 334134 within the 7th European Union Framework Program. T.W.'s PhD is supported though a Collaborative International Research Programme: University of Strathclyde and Nanyang Technological University, Singapore. The authors would like to acknowledge that this work was carried out in part at the EPSRC Future Continuous Manufacturing and Advanced Crystallisation (CMAC) Research Hub (EP/P006965/1), supported by a UK Research Partnership Fund award from the Higher Education Funding Council for England (Grant HH13054).

Declaration: The authors have no conflict(s) of interest to declare.

*Correspondence to: C. Werner, Leibniz Institute of Polymer Research Dresden, Max Bergmann Center of Biomaterials Dresden, 01069 Dresden, Germany.
**Correspondence to: F.P. Seib, Strathclyde Institute of Pharmacy and Biomedical Sciences, University of Strathclyde, Glasgow, G4 0RE, UK.
E-mail addresses: werner@ipfdd.de (C. Werner), philipp.seib@strath.ac.uk, philipp.seib@SeibLab.com (F.P. Seib).

http://dx.doi.org/10.1016/j.nano.2017.07.012

Please cite this article as: Maitz MF, et al, Biocompatibility assessment of silk nanoparticles: hemocompatibility and internalization by human blood cells. *Nanomedicine: NBM* 2017;13:2633-2642, http://dx.doi.org/10.1016/j.nano.2017.07.012

nanoparticles – for example, with hydrophilic poly(ethylene glycol) (PEG) chains – to yield "stealth" nanoparticles, (reviewed in[7,8]). This 'PEGylation' renders nanoparticles more hydrophilic, provides steric hindrance, suppresses protein adsorption from the plasma (for example, the FXIIa-Kallikrein-FXI activation complex) and aggregation by hydrophobic interactions, thereby increasing the nanoparticle circulation time 40- to 90-fold, improving blood compatibility and inhibiting accumulation by the reticuloendothelial system.[6,9] Therefore assessment of "blood performance" is a critical aspect when designing nanoparticles for solid tumor targeting.

Pro- or anticoagulant properties of different nanoparticles and their interaction with blood cells generally appear to be at least in part material dependent. Nanosized particles with a diameter below 200 nm, however, frequently have different properties than the corresponding bulk material from which they are derived.[10] The high surface area of nanoparticles supports a pronounced interaction with the biological environment and typically leads to substantial protein adsorption. The conformation of the adsorbed proteins and subsequent protein–protein interactions, in turn, are modified by the high curvature of the nanoparticle, imparted by its small radius.[11-14] For example, polystyrene particles below 20 nm tend to prevent activation of the intrinsic coagulation pathway, because these particles are physically too small to allow assembly of the FXIIa-Kallikrein-FXI activation complex. In contrast, larger particles of the same material show strong pro-coagulant properties.[11,12,14] Therefore knowledge of bulk material properties does not predict nanoparticle blood compatibility; as consequence nanoparticles require hemocompatibility assessment.

One promising biopolymer material for nanoparticle-mediated drug delivery is silk, which is characterized by (i) an excellent track record in humans, (ii) unique physical properties, (iii) mild processing conditions, (iv) the ability to adopt a broad range of material formats, and (v) a capacity for stabilizing therapeutic proteins and small-molecular drugs.[15,16] For example, we have recently developed macroscopic silk films,[17-19] hydrogels[20] and nanoparticles[21,22] for the treatment of neuroblastoma and breast cancer. A broad range of manufacturing processes have been used to generate silk nanoparticles; for example, milling, emulsification, salting out, organic solvent precipitation, supercritical CO_2, and capillary microdot printing (reviewed in[23]). These manufacturing approaches induce extensive β-sheets within the crystalline regions of the silk heavy chain resulting in tightly packed and stable silk nanoparticles.[15] Silk nanoparticles generated from *Bombyx mori*, *Antheraea mylitta,* and recombinant spider silks [24-28] are typically endowed with an excellent drug loading capacity and favorable pH dependent release profiles[21] that can be exploited for lysosomotropic drug delivery (reviewed in[16]). However, the clinical success of any silk-based nanoparticle will depend on its hemocompatibility.[16] A number of studies have examined the hemocompatibility of *Bombyx mori* silk using macroscale planar silk surfaces.[29-32] These studies have indicated minimal coagulant but substantial complement activation.[31,32] Nonetheless, a direct transfer of the results obtained from macroscopic surfaces to nanoparticles is not appropriate because of the previously mentioned specific and non-typical interactions of nanoparticles with blood.[33,34] Furthermore, hemocompatibility requirements for nanoparticles in the blood circulation appear even more stringent than those for solid surfaces because any incompatibility reaction of systemically administered nanoparticles would affect multiple organs.

To date, nanoparticle hemocompatibility studies have mainly been restricted to bare and surface-modified iron oxide, poly(lactic-*co*-glycolic acid), silica, polystyrene, and carbon nanotubes.[12,14,34-36] Overall, these studies typically provide an incomplete snapshot because (i) the measurements are performed under static incubation conditions, which facilitates nanoparticle aggregation, (ii) physiological shearing forces are excluded, (iii) the measurements are performed using non-human blood, (iv) "hemocompatibility" assessment often consists of simple hemolysis assays, and (v) differential measurements that interrogate the complement and coagulation cascades are lacking.

The hemocompatibility for as yet uncharacterized nanoparticles, including silk nanoparticles, remains obscure, largely due to the limited knowledge of bulk material properties. Our aim in the present study was to test the hemocompatibility of silk nanoparticles (both native and PEGylated) and directly compare their performance to that of well-characterized silica nanoparticles. For these studies, we exposed human whole blood to quasi-static conditions as well as to flow conditions that mimic *in vivo* shear forces, and we complemented these studies with single-cell live cell imaging to assess the cellular uptake of nanoparticles.

Methods

Nanoparticles

Silica nanoparticles were purchased from NanoComposix, Inc. (San Diego, CA, USA) as both bare and NH_2 functionalized particles with a physical diameter of 101.7 nm (± 9 nm) and 101.5 nm (± 7.4 nm), respectively. Stock suspensions in ultrapurified water were prepared at a concentration of 5 mg/ml. Silk nanoparticles were prepared in a one-step nanoprecipitation procedure, as described previously[21,22] and detailed in the Supplementary Material section; for a visual protocol format see.[37] The methodologies for assessing nanoparticle size, charge, morphology and sedimentation behavior are detailed in the Supplementary Material.

Endotoxin testing

Surface adsorbed endotoxin was eluted from the nanoparticles based on the method by Maitz[38] and is detailed in the Supplementary Material.

Human whole blood incubation assays

All studies were approved by the ethics board and complied with institutional and international guidelines (review board of Technische Universität Dresden, Germany). All blood donors provided informed consent. Studies were performed with at least one independent repeat, and both runs contained triplicate sets of samples and donors were selected similar to previous studies[31,32] and detailed in the Supplementary Material.

Nanoparticle uptake studies using whole and fractionated blood

Endocytic uptake of fluorescently labeled nanoparticles in whole blood was determined using a quasi-static 2 h incubation at both 37 °C and at 4 °C. The experimental method is detailed in the Supplementary Material.

Statistical analyses

Data analysis is detailed in the Supplementary Material.

Results

Nanoparticle characterization

Scanning electron microscopy confirmed that all nanoparticles were spherical and had the expected sizes and surface charge (in water): native silk nanoparticles (106.1 nm ± 0.8, zeta potential −53 mV ± 1.7), PEGylated silk nanoparticles (116.1 nm ± 0.2, zeta potential −43.6 mV ± 2.8), native silica nanoparticles (101.7 nm ± 9.0, zeta potential −31.8 mV ± 0.3), and amine functionalized silica nanoparticles (101.5 nm ± 7.4, zeta potential −16.1 mV ± 0.6). Exposure of silk nanoparticles to 100 mM phosphate buffered saline (PBS) substantially increased the native silk nanoparticle size over time, whereas no changes were observed for PEGylated silk nanoparticles (Supplementary Figure 1). Exposure of native silk nanoparticles to 10% v/v fetal bovine serum (FBS) reduced the PBS-mediated particle aggregation; this aggregation did not occur with PEGylated silk nanoparticles (Supplementary Figure 1). Native and amine-functionalized silica nanoparticles showed increased particle size over time in response to increased buffer strength. Inclusion of FBS reduced this apparent silica nanoparticle aggregation (Supplementary Figure 1). Native and PEGylated silk nanoparticles showed no signs of aggregation in water, whereas both native and amine-functionalized nanoparticles showed similar particle sedimentation characteristics (Supplementary Figure 2). The colloidal stability of silk nanoparticles has been reported previously.[22]

Endotoxin contamination of nanoparticles

Endotoxin contamination is a frequent issue with nanoparticles and can confound the results of hemocompatibility studies.[38] The detergent-mediated endotoxin release from all 250 μg/ml nanoparticle suspensions was well below the reported US Food and Drug Administration threshold value of 0.5 EU/ml for eluates of biological products and medical devices (Figure 1).[39] Silica and silica-NH_2 nanoparticles released only marginal amounts of LPS, at 0.007 and 0.02 EU/ml, respectively. Native and PEGylated silk nanoparticles released 0.12 EU/ml and 0.05 EU/ml, respectively. Therefore, all nanoparticle preparations were well within the acceptable limits for LPS eluates. We spiked nanoparticles with 0.5 EU/ml of LPS and determined subsequent LPS recovery. Recovery for native silk nanoparticles was complete, while PEGylated silk nanoparticles were able to quench about 50% of the spiked LPS. Silica and silica-NH_2 nanoparticles quenched 70% and 80% of the spiked LPS, respectively.

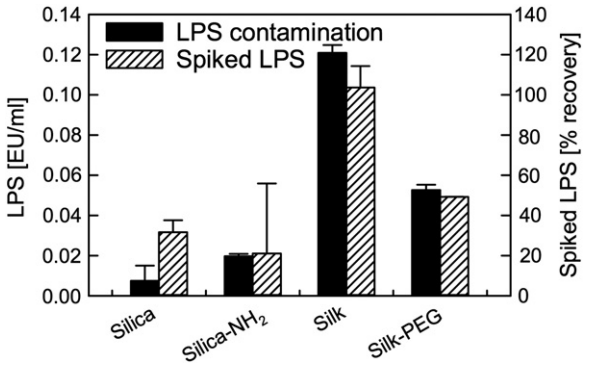

Figure 1. Endotoxin contamination of nanoparticles. Amount of lipopolysaccharides (LPS) extracted from 250 μg nanoparticle samples using a 1 ml aqueous 0.2% v/v Tween-20 extraction buffer. LPS recovery for nanoparticles spiked with 0.5 EU LPS. The threshold for eluates from medical devices has a limit of 0.5 EU/ml. (mean ± SD, n = 2 independent measurements).

Dose dependent effects of nanoparticles on coagulation and inflammation

First, we examined the impact of nanoparticle dose on hemocompatibility. Whole blood was incubated for two hours with native silica, amine-functionalized silica, and native silk nanoparticles at concentrations of 2.5, 25, and 250 μg/ml in reaction tubes under quasi-static conditions. Next, blood samples were tested for hemostasis and inflammation biomarkers (Figure 2).

At the lowest nanoparticle concentration of 2.5 μg/ml, no coagulation activation was detected using prothrombin F1 + 2 fragment as biomarker (Figure 2, *A*). At the higher nanoparticle concentrations, the native silica nanoparticles induced a dose-dependent increase in activation and coagulation; at a nanoparticle concentration of 250 μg/ml silica dosed samples were significantly different from the control ($P < 0.01$). This dose-dependent activation was completely abolished for amine-functionalized silica nanoparticles. The silk nanoparticles induced dose-dependent coagulation activation; a significant difference was observed at a nanoparticle concentration of 250 μg/ml when compared to the water control (Figure 2, *A*).

Blood platelet activation, measured as platelet factor 4 (PF4) release, showed only minor dose dependence for the various nanoparticles: a 100-fold dose increase of silica or silk nanoparticles induced a 2.6- and 2.8-fold increase of PF4 release, respectively (Figure 2, *B*). Aminated silica nanoparticles did not activate blood platelets but instead appeared to suppress platelet activity at high nanoparticle concentrations. In contrast, native silk nanoparticles showed significant dose dependent platelet activation when compared to the controls. PF4 release correlated well with the decay of blood platelets during the incubation (Supplementary Figure 3).

The C5a fragment of the common complement pathway was measured and served as a total complement activation marker (i.e. without discriminating its initiation by the classical or alternative route). Complement activation exhibited only minor dose dependence for all studied nanoparticles: the C5a level increased only two-fold for aminated silica and native silk nanoparticles and four-fold for native silica nanoparticles, despite a 100-fold increase

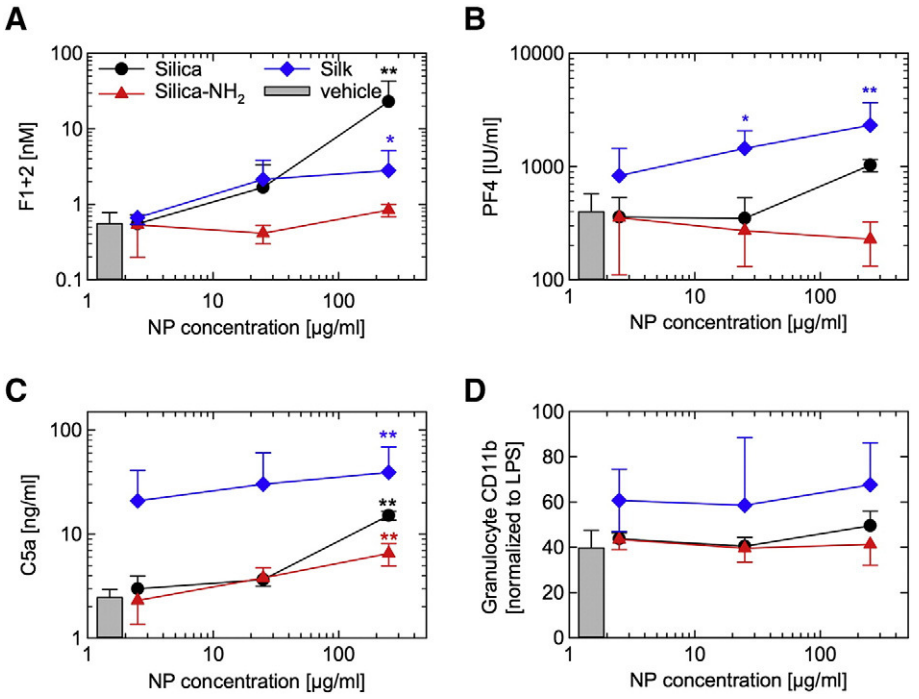

Figure 2. Activation of hemostasis and inflammation parameters of human whole blood in response to different nanoparticle concentrations. Nanoparticles were added to 1.5 U/ml heparinized blood and incubated for 2 h under quasi-static incubation conditions while avoiding sample sedimentation. (A) Prothrombin fragment F1 + 2 as a marker for plasmatic coagulation. (B) Platelet factor 4 (PF4) as a marker for platelet activation. (C) Complement fragment C5a as a marker for complement activation. (D) Granulocyte CD11b expression as a marker for leukocyte activation. Vehicle: ultrapure water; the continuous phase used for nanoparticle preparations. Mean ± SD of n = 6; asterisks indicate significant difference to the water control (*: $P < 0.05$; **: $P < 0.01$).

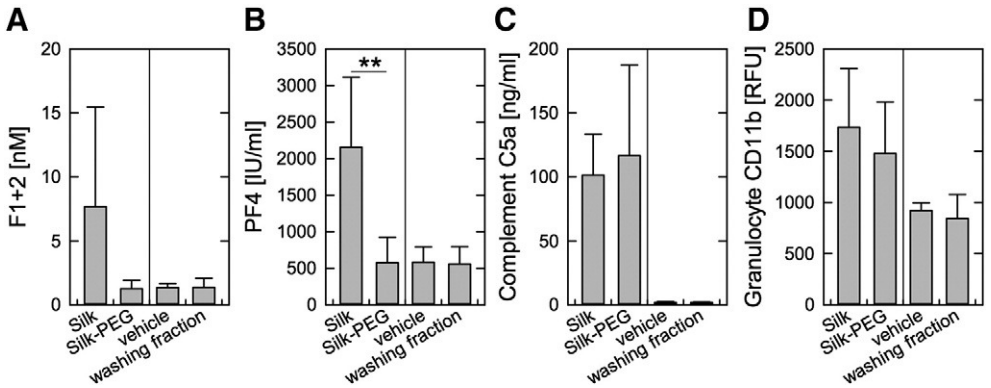

Figure 3. Impact of PEGylation on silk nanoparticle hemocompatibility. Activating effect of silk nanoparticles (250 µg/ml) on human whole blood. Nanoparticles were added to 1.5 U/ml heparinized blood and incubated for 2 hours under quasi-static incubation conditions while avoiding sample sedimentation. Hemostatic activity (F1 + 2 fragment and PF4 release, panels A and B, respectively) and pro-inflammatory response (C5a and granulocyte activation, panels C and D, respectively) of native and PEGylated silk nanoparticles. The final aqueous washing fraction generated during silk nanoparticle preparation. Vehicle: ultrapure water; the continuous phase used for nanoparticle preparations. (mean ± SD of n = 6).

in nanoparticle concentration (Figure 2C). No significant differences were noted in complement activation between native and amine-functionalized silica. In contrast, native silk particles showed a 10-fold higher complement activation than the control, although silk nanoparticles showed no significant dose dependence in the analyzed range. In agreement with complement activation results (Figure 2, *C*), leukocyte activation, measured as granulocyte CD11b expression (Figure 2, *D*), was elevated in response to addition of silk nanoparticles but showed no dose dependence for any of the tested nanoparticles.

The high baseline platelet and inflammatory activation observed for native silk nanoparticles was not attributable to compound(s) and/or contaminants that could be readily leached from silk nanoparticles, because collection and analysis of the final washing fraction generated during silk nanoparticle preparation did not induce this activation (Figure 3). Indeed,

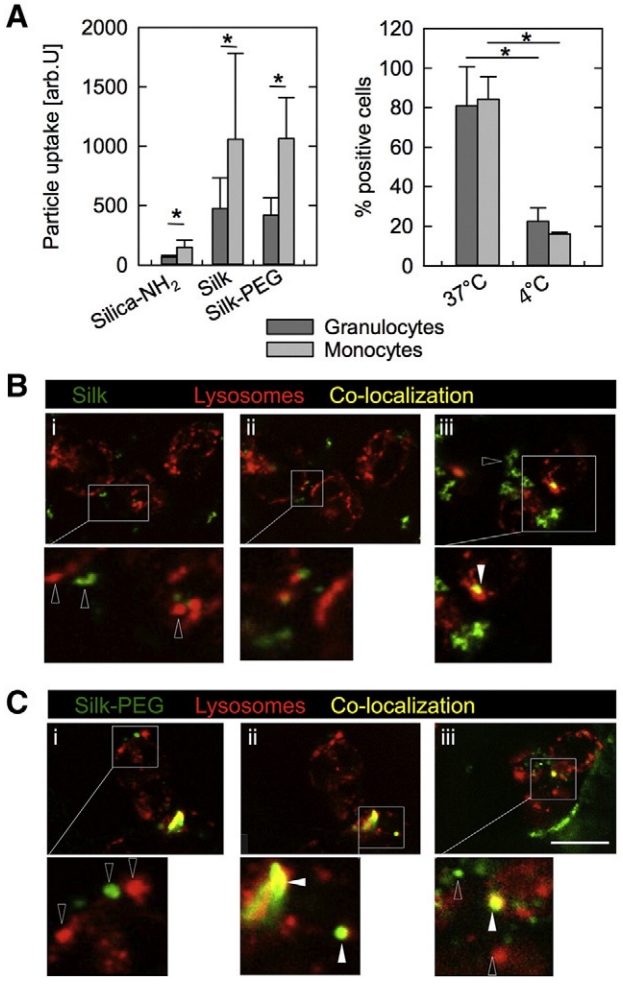

Figure 4. Cellular uptake of silk nanoparticles. (A) Nanoparticles were incubated with human whole blood for 2 h and cell-associated fluorescence of granulocytes and monocytes was assessed by flow cytometry. Silk-nanoparticle positive cells after 2 h incubation with native silk nanoparticles at 37 °C and 4 °C. The 4 °C studies were conducted to estimate plasma membrane nanoparticle binding. Statistically significant differences between samples are indicated by a horizontal line with asterisk ($P < 0.05$; mean ± SD of n = 6). Live cell confocal slices (i–iii) of isolated monocytes incubated for 2 h with (B) native and (C) PEGylated silk nanoparticles. Lysosomes were stained red and silk preparations were green. Open arrows denote single color vesicles (red or green) and closed arrows co-localization (yellow). Scale bar 10 μm.

this washing fraction induced a similar biological response to the one observed for ultrapure water (Figure 3). Therefore, native silk nanoparticles were PEGylated to provide further improvement in silk nanoparticle hemocompatibility. PEGylation suppressed the pro-coagulant characteristics of silk nanoparticles from the pre-existing low level to the levels seen for negative control samples (Figure 3, *A*). Furthermore, silk nanoparticle PEGylation significantly suppressed blood platelet activation ($P < 0.01$) to levels comparable to controls (Figure 3, *A* and *B*). However, levels of the inflammatory markers (C5a fragments and granulocyte CD11b expression) remained high and were not significantly affected by surface decoration of the silk nanoparticles with 5000 g/mol ethoxypolyethylene glycol (Figure 3, *C* and *D*).

Nanoparticle uptake using whole and fractionated blood

Flow cytometry of human whole blood after incubation with fluorescently labeled silk nanoparticles showed cell-associated fluorescence for granulocytes (dim) and monocytes (bright) (Figure 4, *A*). PEGylated silk nanoparticles behaved similarly to native silk nanoparticles. Blood samples incubated with fluorescently labeled aminated silica nanoparticles showed lower cell-associated fluorescence when compared to samples incubated with silk nanoparticles. Furthermore, monocytes incubated with aminated silica nanoparticles appeared brighter than granulocytes (Figure 4, *A*).

Measurements of cell-associated fluorescence by flow cytometry typically do not permit differentiation of internalized (i.e., endocytosed) and non-specific plasma membrane adsorbed nanoparticles. Therefore, in parallel experiments, cells were incubated on ice together with native silk nanoparticles to estimate plasma membrane adsorption of nanoparticles. Four-fold higher numbers of fluorescent cells were observed when incubation was conducted at 37 °C than at 4 °C. Despite the differences in the fluorescence intensity between monocytes and granulocytes (Figure 4, *A*, left graph), no significant difference was noted in the percentage of positive and negative cells at the respective temperatures (Figure 4, *A*, right graph).

Flow cytometry studies were supplemented using live cell fluorescence microscopy of isolated monocytes (Figures 4 and 5). Here, time-lapse studies indicated that native silk nanoparticles started to form microsized aggregates (Figure 5, *B*) in culture and that these aggregates were taken up by monocytes and subsequently released (Figure 5, *A*) or retained (Figure 5, *B* and Supplementary movie 1). Some of these retained silk nanoparticle aggregates were trafficked to acidic vesicles (Figure 4, *B*) within 30 minutes (time-lapse data not shown). The behavior of PEGylated silk nanoparticles differed markedly from that of the native silk nanoparticles, showing less nanoparticle aggregation during the course of the study. In particular PEGylated silk nanoparticles showed vesicular labeling throughout monocyte cytoplasm, in addition to some co-localization with acidic vesicles (Figure 4, *C*).

Shear flow incubation of nanoparticles with whole blood

The quasi-static blood incubation studies were complemented by blood compatibility studies of the nanoparticles under shear conditions in an attempt to better mimic the *in vivo* scenario. Therefore, blood was incubated with 250 μg/ml nanoparticles in a Chandler loop setup[40] at a flow rate of 12 cm/s. Both hemostasis and inflammation biomarkers were monitored and directly compared to the quasi-static incubation setup (Figure 6, *A*).

Many of the datasets for the quasi-static and the Chandler loop experiments were similar. For example, native silica nanoparticles had a high coagulation activation (prothrombin F1 + 2 levels) that was suppressed to baseline levels through silica amination (Figure 6, *B*). This high coagulation activation of native silica nanoparticles was significantly greater than the activation seen for either the native or PEGylated silk nanoparticles (Figure 6, *B*). Under both quasi-static and flow conditions, native silk nanoparticles showed high levels of platelet activation that was matched by the decay in platelet

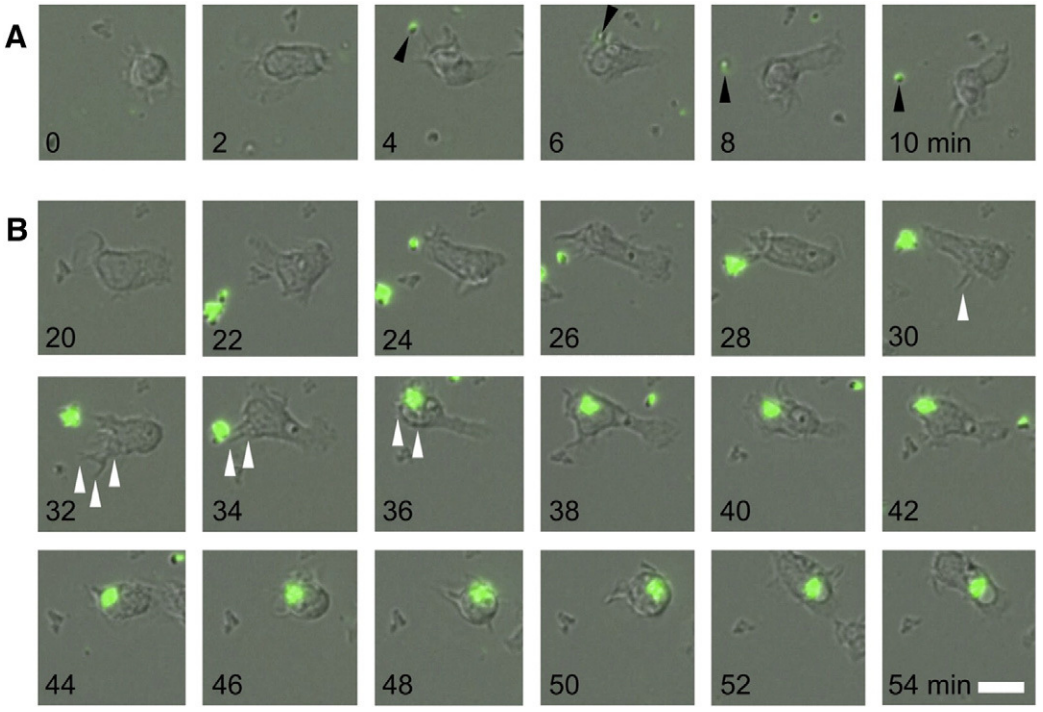

Figure 5. Time-lapse microscopy of a single human monocyte exposed to native silk nanoparticles. (A) Time dependent uptake and subsequent release of silk nanoparticle aggregate (closed black arrow). (B) Retention of a silk nanoparticle aggregate by a monocyte. White arrows show plasma membrane ruffling and subsequent phagocytosis of silk. Monocyte shown in (A) and (B) is the same cell; images are montages of phase contrast and epifluorescent images of a cell and silk (green), respectively. Scale bar 10 μm.

numbers in whole blood (Figure 6, *C*, Supplementary Figure 4). Notably, platelet activation under flow conditions was comparable for both native silk and silica. However, the blood platelet activation seen with silk nanoparticles was significantly suppressed when PEGylated silk nanoparticles were tested under both conditions (Figure 6, *C*). Assessment of CD11b as a marker for granulocyte activation showed similar activation levels for silica nanoparticles and vehicle controls under both quasi-static and flow conditions (Figure 6, *E*). Elevated CD11b levels, were observed for native and PEGylated silk nanoparticles when compared to vehicle controls.

Nevertheless, some striking differences in the results were observed for the two incubation modes: The shear conditions typically induced higher blood platelet activation, based on the PF4 marker (Figure 6, *C*). However, the already very high expression levels of PF4 for native silk nanoparticles under quasi-static conditions resulted in little change under flow conditions. In contrast, the high C5a levels induced by native and PEGylated silk under static conditions were significantly reduced under flow conditions, with little overall change in C5a levels observed for controls and silica, where the C5a levels were already low under static conditions (Figure 6, *D*). Furthermore, under quasi-static conditions native silk nanoparticles showed substantially higher Prothrombin-fragment F1 + 2 than under flow conditions (Figure 6, *B*).

The flow incubation was also performed with fluorescently labeled silk nanoparticles. Here, monocytes were subsequently isolated and imaged by fluorescence microscopy (Figure 7). Here, studies with native silk nanoparticles resulted in a loss of monocytes, so that these cells could not be isolated and imaged. However, microscopy of the PEGylated silk nanoparticles showed co-localization of the nanoparticles in lysosomes.

Discussion

Hemocompatibility testing of “nanomedicine” is typically performed under static conditions, often using non-human fractionated blood coupled with endpoint measures, such as hemolysis. These types of studies can be useful for initial screening purposes and provide a first indication of the nanomedicine–blood interaction.[33,34] However, the absence of hemolysis in these studies is often used to classify novel nanomedicine as “hemocompatible”; this undermines our current understanding of hemocompatibility and with potentially deleterious consequences. Note that no hemolysis was evident for the silk nanoparticles studied here as well as macroscopic silk films.[29-32] A direct transfer of hemocompatibility properties from the macroscopic material to their nanosized counterparts also is not appropriate. We therefore selected 100 nm nanoparticles for this study because this size is particularly relevant for anticancer nanomedicines. For example, emerging (e.g., BIND-014) and clinically used anticancer nanomedicines (e.g., Doxil) are within this 100 nm size range, while larger nanoparticles (e.g., >200 nm) are currently not undergoing clinical development because the optimum nanoparticle size for solid tumor targeting via the EPR effect is in the 100 nm size range and below.[2]

Some isolated hemostasis or inflammatory reactions have been reported for nanoparticles in general,[34] but these studies typically disregard the interplay of inflammatory and hemostatic, humoral,

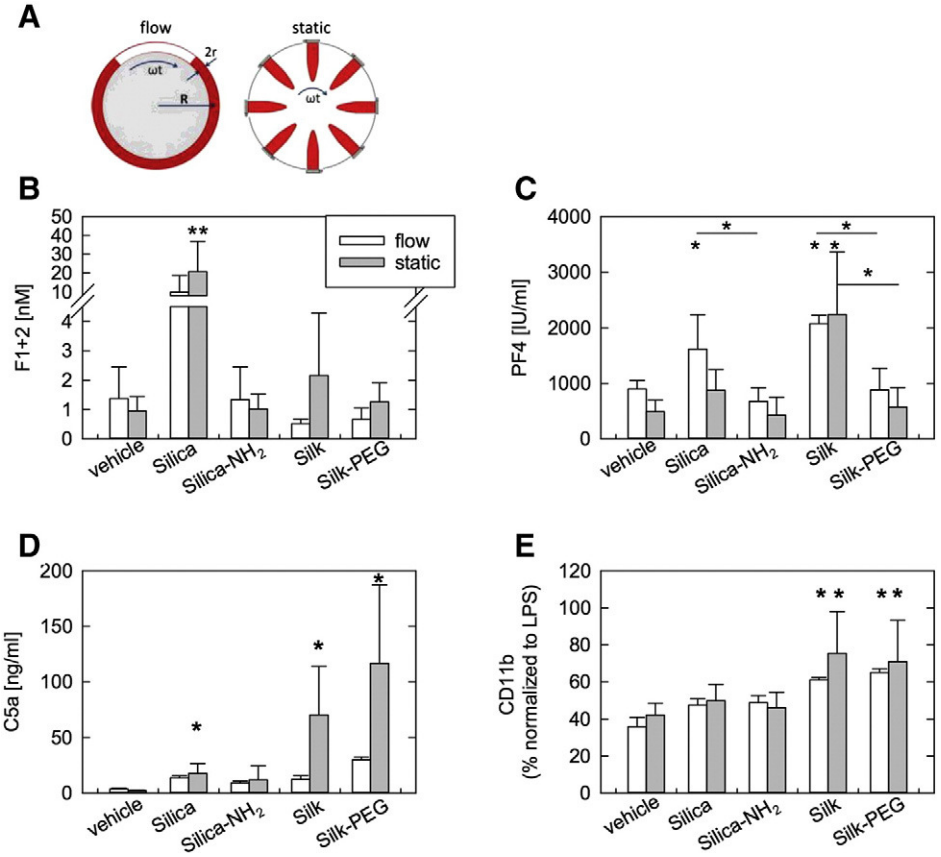

Figure 6. Impact of flow on nanoparticle hemocompatibility in human whole blood. (A) Scheme of the flow and quasi-static setup. A flow of 12 cm/s was obtained in a rotating closed loop system (Chandler loop); the quasi-static incubation was conducted in reaction tubes under constant overhead rotation. (B–E) Coagulation and inflammation activation of whole blood dosed with nanoparticles and incubated for 2 h under flow or quasi-static conditions. Prothrombin-fragment F1 + 2, platelet factor 4 (PF4), complement C5a concentration, and granulocyte CD11b expression level were used as biomarkers for blood activation. Mean ± SD of n ≥ 6. Asterisks above a column indicate significant difference to the water blank; differences between samples are indicated by a horizontal line with asterisk ($P < 0.05$).

and cellular systems as well as the impact of flow conditions. Hemocompatibility testing of nanoparticles rarely includes the use of human whole blood and flow conditions.[41] In the current study, our aim was to compare our well established human whole blood hemocompatibility setup[42,43] with a state-of-the-art dynamic incubation protocol and live cell imaging. We used these test systems to compare the inflammatory and hemostasis response of novel silk nanoparticles and previously well-characterized silica nanoparticles.

We and others have recently reported the use of silk nanoparticles for anticancer drug delivery, in particular for targeting to solid tumors[21,22,27,44] and their ability to reprogram macrophage metabolism.[45] However, little is known about silk nanoparticle performance in the bloodstream. We therefore assessed native and PEGylated silk nanoparticles and compared their performance directly with well-established silica nanoparticles using a range of test systems. Native silk nanoparticles, at the lowest concentration of 2.5 μg/ml, induced higher blood platelet (PF4), leukocyte (CD11b expression) and complement (C5a) activation than was observed in the blank control, whereas native and aminated silica nanoparticles at this concentration induced activation levels similar to the control (Figure 2). In a separate set of studies, where all nanoparticles were subjected to a washing protocol to estimate the potential contribution of LPS contamination to overall hemocompatibility, the observed blood activation was a direct consequence of the nanoparticles and was not due to elution of soluble substances (Figure 1).

The maximum nanoparticle concentration used in the present study was 250 μg/ml; this concentration was based on estimates for using silk nanoparticles as a doxorubicin drug delivery system (i.e., 40 ng doxorubicin/μg silk). Assuming a human blood volume of 5 liters, a nanoparticle concentration of 250 μg/ml is a reasonable estimate at steady state. We used the maximum concentration of 250 μg/ml and tested the dose dependence of coagulant and inflammatory responses of nanoparticles over two orders of magnitude. For all parameters tested, only a sublinear response was observed. At most, the 100-fold increase in silica nanoparticle concentration caused a 40-fold increase in the thrombin activation (Figure 2, *A*). For other parameters and other materials, the increase was less significant. We compared nanoparticle performance based on mass rather than nanoparticle numbers. When based on the nanoparticle numbers, we used approximately 30% more silk nanoparticles than silica nanoparticles. Dose–response studies indicated that, typically, a > 200% increase in nanoparticle number was required to induce any substantial biological change (Figure 2).

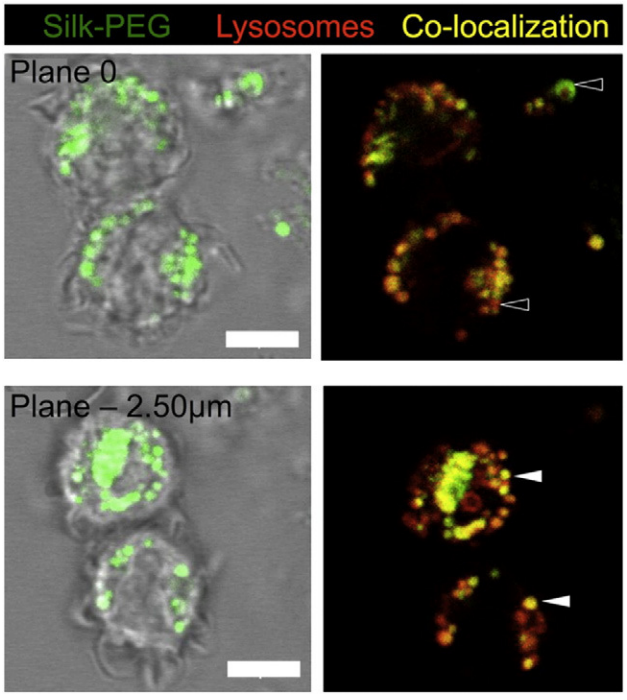

Figure 7. Impact of flow on PEGylated silk nanoparticle uptake and trafficking in human whole blood. Whole blood was incubated with PEGylated silk nanoparticles for 2 h under dynamic conditions followed by immediate monocyte isolation, lysosome staining and imaging of live cells. Lysosomes were stained red and PEGylated silk nanoparticles were green. Open arrows denote single color vesicles (red or green) and closed arrows co-localization (yellow). Images are montages of phase contrast and confocal slices at two focal planes. Scale bar 5 µm.

A potential caveat of our study is that we cannot exclude the possibility of nanoparticle aggregation decreasing the effective surface area (Supplementary Figures 1 and 2), thereby leading to the non-linear response. High PF4 and C5a levels observed over the particle concentration test range might indicate saturation and/or exhaustion.

Different types of nanoparticles and nanotubes activate blood platelets at concentrations above 20 µg/ml via a plasma membrane Ca^{2+} flux dependent pathway.[46,47] Lower concentrations of the nanoparticles sensitize platelets to thromboxane (TxA_2) and ADP.[46] The results reported here for native silica particles were in good agreement with the literature, whereas the threshold for native silk nanoparticles to induce blood platelet activation appeared to be below 2.5 µg/ml. Thrombin generally is the strongest activator of blood platelets, and platelet activation in hemocompatibility tests typically closely correlates with thrombin formation. The current study strongly suggests that the native silk nanoparticles activated platelets directly, because thrombin formation was not observed (Figure 3).

Despite a number of blood studies examining silk hemocompatibility[29-32] the underlying mechanism(s) of cell and humoral pathway activation by silk remains to be elucidated. Previous studies using macroscopic silk films also demonstrated that silk directly activated platelets.[31,32] Notably, the overall blood compatibility performance was not dependent on a single factor (e.g., silk secondary structure), but on a multitude of processing parameters.[32] We therefore cannot speculate which silk nanoparticle feature contributes to its overall hemocompatibility performance.

Silk is known for inducing a mild inflammatory response *in vivo*.[48] We previously observed a substantial *in vitro* complement activation of the alternative pathway with macroscopic silk films and human whole blood.[31,32] Complement activation requires the assembly of multi-enzyme complexes on the foreign surface. Several studies have shown that complement activation by IgM via the classical pathway is geometrically hindered on small nanoparticles with diameters below 250 nm, because for these particles the curvature is too high and the available area too small for the assembly of the complement complexes.[49,50] Few studies have examined the ability of nanoparticles to activate the complement system via the alternative pathway. The initiator of this alternative pathway, C3b, occupies a surface area of 40 nm^2, suggesting that a relatively large particle with sufficient surface area is required for the successful activation of the complement cascade and propagation to the membrane attack complex.[49,51] In the present study, silk nanoparticles induced high complement activation during static incubation, but complement activation was significantly suppressed in the Chandler-loop incubation (Figure 5). This may be evidence of nanoparticle aggregation during the static incubation, where large nanoparticle agglomerates could be supporting the propagation of the complement cascade. In contrast, in the dynamic studies, the particles conceivably could have remained more dispersed (Supplementary Figures 1 and 2) and the complement cascade did not proceed to completion.

Strong complement activation by nanoparticles may pose a problem for their routine application as nanomedicine, as it may cause complement-dependent allergic reactions that in turn necessitate pre-treatment with steroids.[52] The present study suggests that this systemic effect would be absent for silk nanoparticles, as the complement activation under flowing conditions was substantially diminished. However, aggregation of nanoparticles remains a conceivable possibility in the extracellular space of solid tumors, with the potential to activate the complement system there. Induction of complement activation via anticancer nanomedicine is a significant problem, because the C5a anaphylatoxin is known to stimulate tumor growth by suppression of CD8 T-cells.[53-55] In turn, blockage of C5a signaling decreases tumor growth with efficiency similar to that of paclitaxel-based anticancer treatment.[53] Therefore, minimizing nanoparticle aggregation is critical for their development as nanomedicine.

Stealth technologies such as PEGylation are typically used to prevent nanoparticle aggregation and to minimize their detrimental interactions with biological systems. In the present study, PEGylated silk nanoparticles efficiently suppressed coagulation and blood platelet activation (Figure 3, *A* and *B*). Furthermore, PEGylated silk nanoparticles also showed less aggregation under static conditions (Figure 4, *C*). Nevertheless, complement and leukocyte activation persisted, although complement-activating free hydroxyl groups were avoided with the use of monomethoxy terminated PEG.[22,42] PEGylation not only improves colloidal stability[22] and blood compatibility, but it also reduces serum protein adsorption. Consequently, PEGylated silk

nanoparticles are expected to have a reduced and/or different biomolecular corona when compared to native silk nanoparticles. This biomolecular corona is expected to influence (silk) nanoparticle performance.[56] However, little is known at present regarding the extent and the composition of the biomolecular corona for silk nanoparticles.

In whole blood, both silica and silk nanoparticles were actively taken up by granulocytes and monocytes, with monocytes showing the highest nanoparticle uptake (Figure 4). However, the low abundance of monocytes in the blood meant that only approximately 20% of the total nanoparticle uptake could be attributed to those cells. The literature examining nanoparticle uptake by blood cells is sparse: monocytes are frequently seen as the most important cell type responsible for nanoparticle uptake in blood and are thus considered during (nano)particle design.[57] Granulocytes, by contrast, are rarely the focus of attention when designing novel nanomedicines.[58] We attempted to differentiate between plasma membrane associated nanoparticle fluorescence and endocytosed nanoparticles by performing incubation studies at 4°C and 37°C, respectively. The incubation studies on ice verified that the majority of cell-associated fluorescence was due to active uptake by the cells rather than non-specific plasma membrane binding of nanoparticles; this was independent of the cell type.

Endocytic uptake was also verified by live cell fluorescence microscopy studies using both native and PEGylated silk nanoparticles and isolated monocytes. The PEGylated silk nanoparticles showed clear evidence of an endocytic accumulation into acidic, LysoTracker positive vesicles, which were most likely lysosomes. This intracellular pattern of silk nanoparticle accumulation correlates well with studies that examined endocytosis of silk nanoparticles in breast cancer cells.[21,22] However, the exact endocytic uptake mechanism(s) by human monocytes remains to be determined.[16]

Many nanomedicines are traditionally designed for targeting of solid tumors, and especially cancer cells. However, we have demonstrated here that they can directly interact with subpopulations of blood cells. Therefore, nanoparticles can conceivably evoke unintended responses in these cells during their journey to their final tumor destinations. Alternatively, recent evidence suggests that particulate-mediated immune modulation of inflammatory monocytes can be exploited to moderate inflammatory responses in a broad spectrum of diseases.[59] Thus the appropriate design of a particulate (nano)medicine is critical to achieve the intended outcome.[60]

We demonstrated substantial differences for selected nanomedicines in quasi-static and dynamic hemocompatibility studies. In particular, the inflammatory response was significantly reduced for silk nanoparticles under dynamic conditions when compared to the quasi-static setup. Furthermore, we demonstrated that the silk nanoparticles had very low procoagulant properties, an observation that was scalable from the macroscopic level of planar surfaces to the nano-level.[32] Hemocompatibility studies using silica and silk nanoparticles were complemented by preliminary live cell measurements to provide a first insight into the endocytosis and trafficking of these particles in blood cells. Overall, this study demonstrates that a multitude of factors affect hemocompatibility; thus, the design of the most appropriate test bed for hemocompatibility studies is highly application dependent.

Acknowledgment

We thank Monique Marx for her assistance with the blood incubation assays.

Appendix A. Supplementary data

Supporting Information is available online. All data created during this research are openly available from the University of Strathclyde-Pure, UK Data Service at http://dx.doi.org/10.15129/b00c1d6c-32b6-4724-8e5a-da7e60feafa7. Supplementary data associated with this article can be found in the online version, at http://dx.doi.org/10.1016/j.nano.2017.07.012.

References

1. Duncan R, Gaspar R. Nanomedicine(s) under the microscope. *Mol Pharm* 2011;**8**:2101-41.
2. Shi J, Kantoff PW, Wooster R, Farokhzad OC. Cancer nanomedicine: progress, challenges and opportunities. *Nat Rev Cancer* 2017;**17**:20-37.
3. Maeda H, Nakamura H, Fang J. The EPR effect for macromolecular drug delivery to solid tumors: Improvement of tumor uptake, lowering of systemic toxicity, and distinct tumor imaging in vivo. *Adv Drug Deliv Rev* 2013;**65**:71-9.
4. Xu X, Ho W, Zhang X, Bertrand N, Farokhzad O. Cancer nanomedicine: from targeted delivery to combination therapy. *Trends Mol Med* 2015;**21**:223-32.
5. Dierendonck M, De Koker S, Vervaet C, Remon JP, De Geest BG. Interaction between polymeric multilayer capsules and immune cells. *J Control Release* 2012;**161**:592-9.
6. Petros RA, DeSimone JM. Strategies in the design of nanoparticles for therapeutic applications. *Nat Rev Drug Discov* 2010;**9**:615-27.
7. Pasut G, Veronese FM. State of the art in PEGylation: the great versatility achieved after forty years of research. *J Control Release* 2012;**161**:461-72.
8. Rabanel JM, Hildgen P, Banquy X. Assessment of PEG on polymeric particles surface, a key step in drug carrier translation. *J Control Release* 2014;**185**:71-87.
9. Jokerst JV, Lobovkina T, Zare RN, Gambhir SS. Nanoparticle PEGylation for imaging and therapy. *Nanomedicine* 2011;**6**:715-28.
10. Nel A, Xia T, Madler L, Li N. Toxic potential of materials at the nanolevel. *Science* 2006;**311**:622-7.
11. Kushida T, Saha K, Subramani C, Nandwana V, Rotello VM. Effect of nano-scale curvature on the intrinsic blood coagulation system. *Nanoscale* 2014;**6**:14484-7.
12. Mayer A, et al. The role of nanoparticle size in hemocompatibility. *Toxicology* 2009;**258**:139-47.
13. Oslakovic C, Cedervall T, Linse S, Dahlback B. Polystyrene nanoparticles affecting blood coagulation. *Nanomedicine* 2012;**8**:981-6.
14. Sanfins E, Augustsson C, Dahlback B, Linse S, Cedervall T. Size-dependent effects of nanoparticles on enzymes in the blood coagulation cascade. *Nano Lett* 2014;**14**:4736-44.
15. Seib FP, Kaplan DL. Silk for drug delivery applications: opportunities and challenges. *Isr J Chem* 2013;**53**:756-66.
16. Seib FP. Silk nanoparticles—an emerging anticancer nanomedicine. *AIMS Bioeng* 2017;**4**:239-58.

17. Seib FP, Kaplan DL. Doxorubicin-loaded silk films: drug-silk interactions and in vivo performance in human orthotopic breast cancer. *Biomaterials* 2012;**33**:8442-50.
18. Chiu B, et al. Surgery combined with controlled-release doxorubicin silk films as a treatment strategy in an orthotopic neuroblastoma mouse model. *Br J Cancer* 2014;**111**:708-15.
19. Seib FP, et al. Focal therapy of neuroblastoma using silk films to deliver kinase and chemotherapeutic agents in vivo. *Acta Biomater* 2015;**20**:32-8.
20. Seib FP, Pritchard EM, Kaplan DL. Self-assembling doxorubicin silk hydrogels for the focal treatment of primary breast cancer. *Adv Funct Mater* 2013;**23**:58-65.
21. Seib FP, Jones GT, Rnjak-Kovacina J, Lin Y, Kaplan DL. pH-dependent anticancer drug release from silk nanoparticles. *Adv Healthc Mater* 2013;**2**:1606-11.
22. Wongpinyochit T, Uhlmann P, Urquhart AJ, Seib FP. PEGylated Silk Nanoparticles for Anticancer Drug Delivery. *Biomacromolecules* 2015;**16**:3712-22.
23. Zhao Z, Li Y, Xie MB. Silk fibroin-based nanoparticles for drug delivery. *Int J Mol Sci* 2015;**16**:4880-903.
24. Gupta V, Aseh A, Rios CN, Aggarwal BB, Mathur AB. Fabrication and characterization of silk fibroin-derived curcumin nanoparticles for cancer therapy. *Int J Nanomedicine* 2009;**4**:115-22.
25. Kundu J, Chung YI, Kim YH, Tae G, Kundu SC. Silk fibroin nanoparticles for cellular uptake and control release. *Int J Pharm* 2010;**388**:242-50.
26. Lammel AS, Hu X, Park SH, Kaplan DL, Scheibel TR. Controlling silk fibroin particle features for drug delivery. *Biomaterials* 2010;**31**:4583-91.
27. Tian Y, Jiang X, Chen X, Shao Z, Yang W. Doxorubicin-loaded magnetic silk fibroin nanoparticles for targeted therapy of multidrug-resistant cancer. *Adv Mater* 2014;**26**:7393-8.
28. Zhang YQ, et al. Formation of silk fibroin nanoparticles in water-miscible organic solvent and their characterization. *J Nanopart Res* 2007;**9**.
29. Motta A, et al. Silk fibroin processing and thrombogenic responses. *J Biomater Sci Polym Ed* 2009;**20**:1875-97.
30. Motta A, Migliaresi C, Lloyd AW, Denyer SP, Santin M. Serum Protein Absorption on Silk Fibroin Fibers and Films: Surface Opsonization and Binding Strength. *Bioact Compat Polym* 2002;**17**:23-35.
31. Seib FP, et al. Multifunctional silk-heparin biomaterials for vascular tissue engineering applications. *Biomaterials* 2014;**35**:83-91.
32. Seib FP, Maitz MF, Hu X, Werner C, Kaplan DL. Impact of processing parameters on the haemocompatibility of Bombyx mori silk films. *Biomaterials* 2012;**33**:1017-23.
33. Ilinskaya AN, Dobrovolskaia MA. Nanoparticles and the blood coagulation system. Part I: benefits of nanotechnology. *Nanomedicine* 2013;**8**:773-84.
34. Ilinskaya AN, Dobrovolskaia MA. Nanoparticles and the blood coagulation system. Part II: safety concerns. *Nanomedicine* 2013;**8**:969-81.
35. Chouly C, et al. In vitro study of the hemocompatibility of superparamagnetic contrast agent for magnetic resonance imaging. *Clin Mater* 1994;**15**:293-301.
36. Pham BT, et al. The interaction of sterically stabilized magnetic nanoparticles with fresh human red blood cells. *Int J Nanomedicine* 2015;**10**:6645-55.
37. Wongpinyochit T, Johnston BF, Seib FP. Manufacture and drug delivery applications of silk nanoparticles. *J Vis Exp* 2016:e54669.
38. Maitz MF, Teichmann J, Sperling C, Werner C. Surface endotoxin contamination and hemocompatibility evaluation of materials. *J Biomed Mater Res B Appl Biomater* 2009;**90**:18-25.
39. Administration USFaD Guideline on validation of the limulus amebocyte lysate test as an end-product endotoxin test for human and animal parenteral drugs, biological products and medical devices; 1987.
40. Chandler AB. In vitro thrombotic coagulation of the blood; a method for producing a thrombus. *Lab Invest* 1958;**7**:110-4.
41. Krajewski S, et al. Hemocompatibility evaluation of different silver nanoparticle concentrations employing a modified Chandler-loop in vitro assay on human blood. *Acta Biomater* 2013;**9**:7460-8.
42. Sperling C, et al. In vitro blood reactivity to hydroxylated and non-hydroxylated polymer surfaces. *Biomaterials* 2007;**28**:3617-25.
43. Streller U, Sperling C, Hubner J, Hanke R, Werner C. Design and evaluation of novel blood incubation systems for in vitro hemocompatibility assessment of planar solid surfaces. *J Biomed Mater Res B Appl Biomater* 2003;**66**:379-90.
44. Florczak A, Mackiewicz A, Dams-Kozlowska H. Functionalized spider silk spheres as drug carriers for targeted cancer therapy. *Biomacromolecules* 2014;**15**:2971-81.
45. Saborano R, et al. Metabolic reprogramming of macrophages exposed to silk, poly(lactic-co-glycolic acid), and silica nanoparticles. *Adv Healthc Mater* 2017.
46. Guidetti GF, et al. Nanoparticles induce platelet activation in vitro through stimulation of canonical signalling pathways. *Nanomedicine* 2012;**8**:1329-36.
47. Semberova J, et al. Carbon nanotubes activate blood platelets by inducing extracellular Ca2+ influx sensitive to calcium entry inhibitors. *Nano Lett* 2009;**9**:3312-7.
48. Thurber AE, Omenetto FG, Kaplan DL. In vivo bioresponses to silk proteins. *Biomaterials* 2015;**71**:145-57.
49. Pedersen MB, et al. Curvature of synthetic and natural surfaces is an important target feature in classical pathway complement activation. *J Immunol* 2010;**184**:1931-45.
50. Vorup-Jensen T, Boesen T. Protein ultrastructure and the nanoscience of complement activation. *Adv Drug Deliv Rev* 2011;**63**:1008-19.
51. Moghimi SM, et al. Material properties in complement activation. *Adv Drug Deliv Rev* 2011;**63**:1000-7.
52. Hawkins MJ, Soon-Shiong P, Desai N. Protein nanoparticles as drug carriers in clinical medicine. *Adv Drug Deliv Rev* 2008;**60**:876-85.
53. Markiewski MM, et al. Modulation of the antitumor immune response by complement. *Nat Immunol* 2008;**9**:1225-35.
54. Moghimi SM. Cancer nanomedicine and the complement system activation paradigm: anaphylaxis and tumour growth. *J Control Release* 2014;**190**:556-62.
55. Moghimi SM, Farhangrazi ZS. Just so stories: the random acts of anti-cancer nanomedicine performance. *Nanomedicine* 2014;**10**:1661-6.
56. Monopoli MP, Aberg C, Salvati A, Dawson KA. Biomolecular coronas provide the biological identity of nanosized materials. *Nat Nanotechnol* 2012;**7**:779-86.
57. Rodriguez PL, et al. Minimal "Self" peptides that inhibit phagocytic clearance and enhance delivery of nanoparticles. *Science* 2013;**339**:971-5.
58. Wang Z, Li J, Cho J, Malik AB. Prevention of vascular inflammation by nanoparticle targeting of adherent neutrophils. *Nat Nanotechnol* 2014;**9**:204-10.
59. Getts DR, et al. Therapeutic inflammatory monocyte modulation using immune-modifying microparticles. *Sci Transl Med* 2014;**6**:219ra217.
60. Gustafson HH, Holt-Casper D, Grainger DW, Ghandehari H. Nanoparticle uptake: the phagocyte problem. *Nano Today* 2015;**10**:487-510.